

served transition.

In conclusion, the gamma decay information on the weak-coupling multiplet in ^{209}Bi confirms earlier results that the weak-coupling model works extremely well here. It would therefore be of great interest to attempt to understand quantitatively the small deviations observed.

†Work supported by the National Science Foundation and the U. S. Atomic Energy Commission. One of us (JWH) acknowledges a fellowship from the German Academic Exchange Service (DAAD).

*Present address: Sektion Physik der Universität München, Amalienstrasse 54/I, München, Germany.

‡Present address: Niels Bohr Institute, Copenhagen, Denmark.

§On leave from Argonne National Laboratory, Argonne, Ill.

¹J. Alster, Phys. Rev. 141, 1138 (1966), and Phys. Letters 25B, 459 (1967); S. Hinds, H. Marchant, J. H. Bjerregaard, and O. Nathan, Phys. Letters 20, 674 (1966).

²J. C. Hafele and R. Woods, Phys. Letters 23, 579 (1966); J. C. Hafele, Phys. Rev. 159, 996 (1967).

³B. R. Mottelson, J. Phys. Soc. Japan Suppl. 24, 96 (1968).

⁴R. Broglia, J. Damgård, and A. Molinari, Nucl. Phys. 127, 429 (1969).

⁵I. Hamamoto, Nucl. Phys. 126, 545 (1969), and to be published.

⁶The Doppler-shift program was written by S. Baker at Argonne National Laboratory, according to the work of E. Blaugrund, Nucl. Phys. 88, 501 (1966).

⁷Agrees quite well with the recent measurement of $0.57e^2 b^3$ by R. Broglia, J. S. Lilley, R. Perazzo, and W. R. Phillips (to be published) but is about 40% lower than the values reported by J. F. Ziegler and G. A. Peterson [Phys. Rev. 165, 1337 (1968)].

⁸J. S. Lilley and N. Stein, Phys. Rev. Letters 19, 709 (1967); R. Woods, P. D. Barnes, E. R. Flynn, and G. J. Igo, Phys. Rev. Letters 19, 453 (1967); C. Ellegaard and P. Vedelsby, Phys. Letters 26B, 155 (1968).

⁹D. H. Wilkinson, in Nuclear Spectroscopy, edited by F. Ajzenberg-Selove (Academic Press, Inc., New York, 1960), Pt. B, p. 852; C. F. Perdrisat, Rev. Mod. Phys. 38, 41 (1966).

¹⁰F. R. Metzger, Bull. Am. Phys. Soc. 14, 608 (1969).

¹¹A. de-Shalit, Phys. Rev. 122, 1530 (1961).

¹²R. D. Lawson, private communication; A. de-Shalit and I. Talmi, Nuclear Shell Theory (Academic Press, Inc., New York, 1963), p. 134.

¹³J. D. Bowman, F. C. Zawislak, and E. N. Kaufmann, Phys. Letters 29B, 226 (1969).

OBSERVATION OF "PERIPHERAL" BACKWARD MULTIPION PRODUCTION AT 2.15 BeV/c *†

D. Cline, ‡ J. English, R. Terrell, and W. Wilke
University of Wisconsin, Madison, Wisconsin 53706

and

B. Chaudhary, § H. Courant, E. Marquit, and K. Ruddick
University of Minnesota, Minneapolis, Minnesota 55455

(Received 31 July 1969)

Using the Princeton-Pennsylvania Accelerator rapid-cycling bubble chamber in a flash-lamp triggered mode we have observed backward ($\pi^+\pi^-$) and ($\pi^+\pi^-\pi^0$) multipion production in the reaction $\pi^+n \rightarrow pm(\pi)$ at 2.15 BeV/c. The main characteristics of the data are a sharp forward peaking of the proton relative to the incident π^+ direction for all multipion masses below 1100 MeV/c and the strong production of the ω meson. Backward ω production is observed to be more probable than backward ρ production. The sharp forward peaking of the proton in these reactions is suggestive of the dominance of baryon exchange.

The existence of inelastic hadron-induced reactions that are mediated by meson exchanges is well established. Correspondingly, very little information presently exists concerning inelastic reactions mediated by baryon exchange. In this note we present data on the reactions

$$\pi^+n \rightarrow \pi^+\pi^-p, \quad (\pi^+d \rightarrow \pi^+\pi^-pp); \quad (1)$$

$$\pi^+n \rightarrow \pi^+\pi^-\pi^0p, \quad (\pi^+d \rightarrow \pi^+\pi^-\pi^0pp), \quad (2)$$

with the outgoing proton restricted to kinematic configurations with a low momentum transfer be-

tween the incident π^+ and the outgoing proton. The selection of such a configuration is expected to enhance the probability of baryon-exchange dominance of these reactions. The overall purpose of this experiment was to select and study the small class of all π^+d interactions which result in a forward-produced proton having momentum comparable with that of the incident π^+ beam. Reactions (1) and (2) are a subset of this class of events.

The data on Reactions (1) and (2) were collect-

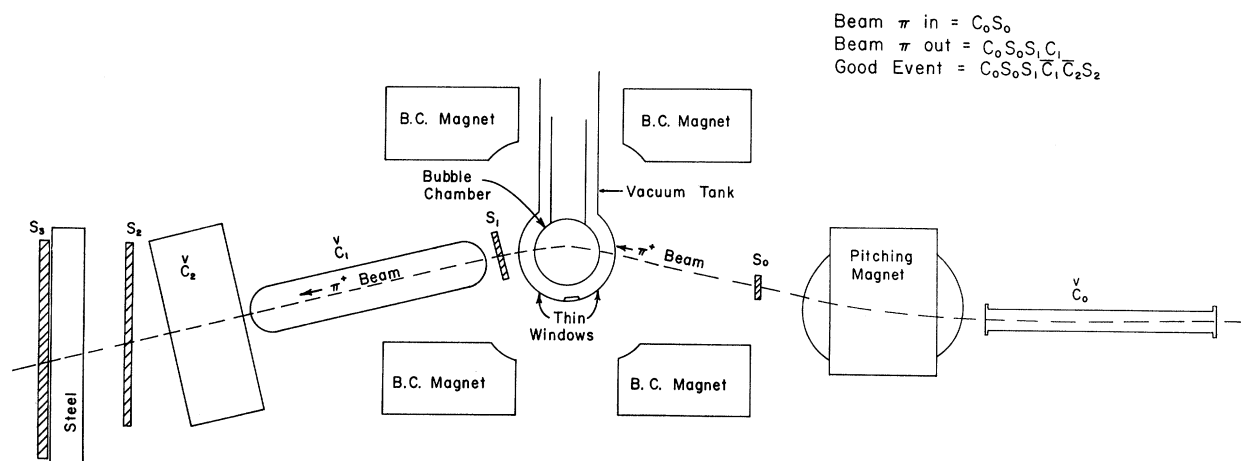


FIG. 1. Experimental setup for Princeton-Pennsylvania Accelerator rapid-cycling bubble chamber with counter control of the lights. C_0 , C_1 , and C_2 are threshold Cherenkov counters.

ed using the Princeton-Pennsylvania Accelerator 14-in. bubble chamber filled with D_2 and exposed to a separated π^+ beam for beam momenta of 1.8, 2.0, 2.15, and 2.4 BeV/c.¹ The magnetic field was run at 18 kG. The bubble chamber was cycled at the rate of 4 to 6 cps and the lights were flashed when a π^+ -induced interaction occurred in the bubble chamber with a fast, forward proton or K^+ leaving the bubble chamber. Figure 1 shows the detection equipment used to select these forward p or K^+ events. Separation of forward protons or K^+ 's from the spray of forward produced π^+ 's is accomplished through the use of two Cherenkov counters C_1 and C_2 . This technique utilizes the reduced velocity of the forward p 's or K^+ 's in comparison with mean velocity of π^+ 's produced in the forward direction. The signature for a probable forward proton or K^+ event was a count in S_1 and S_2 with no count in C_1 or C_2 . Since protons or K^+ 's in the incident beam would also satisfy this signature, an incident π^+ was required to count in the Cherenkov counter C_0 . The occurrence of an event satisfying the above counter signature caused the bubble-chamber lights to be flashed thus recording the event on film. In addition, events for which the forward track traversed 7 in. of steel and counted in S_3 were also recorded. In this latter sample of events it is possible to obtain a lower limit on the momentum of the forward-produced track that traversed S_1 and S_2 without counting in C_1 or C_2 .

In all, 7×10^6 cycles of the bubble chamber were taken and $\sim 75,000$ pictures with events were recorded. The average number of tracks per bubble-chamber cycle was eight. In this note we re-

port on the 2.15-BeV/c part of the experiment which consists of 2.5×10^6 cycles of the bubble chamber.

In order to study Reactions (1) and (2) all three- and four-prong events with a forward-produced positive track were measured. The four-prong events were required to have a visible slow proton identified by ionization. Cuts were imposed on the forward positive track to insure that the particle trajectory could have passed through S_1 in Fig. 1. The standard bubble-chamber analysis programs TVGP-SQUAW were used to reconstruct and kinematically fit the events.² The fitting of Reaction (1) is straightforward involving a four-constraint (4C) or effective 2C fit depending on whether the spectator proton has sufficient momentum to produce a visible track in the bubble chamber. For Reaction (2) the constraint class is lower and the kinematic separation of background is more suspect. In a normal bubble-chamber study such backgrounds would likely swamp the tiny production rate for Reaction (2) (forward-produced protons). However, the restrictive counter-controlled conditions of this experiment lead to the expectation that the background rates will not be prohibitive. Three-prong events not fitting Reaction (1) were fit to Reaction (2) by assuming that the invisible spectator protons have the momentum distribution expected for a Hulthén deuteron wave function. An overall check on the cleanliness of the resulting fits to Reaction (2) was obtained by comparing the number of events with invisible spectators with the number with visible spectators. This ratio is found to be approximately (2-3) in most deuterium bubble-chamber experiments. In our

experiment the ratio is 3.8 ± 0.6 indicating at least a sufficiency test for the separation of Reaction (2) from background. An additional test, to be described below, is the observation of the production of known narrow resonances in such a reaction. Since the ω meson decays into $\pi^+\pi^-\pi^0$, the clean observation of this state at the correct mass is further evidence for the reliability of the separation of Reaction (2) from background.

We now turn to a discussion of the events fitting Reactions (1) and (2). Events for Reaction (1) with the π^+p mass in the range of 1200-1300 were removed to exclude the $\Delta^{++}\pi^-$ final state.³ The same cut was applied to Reaction (2) to remove $\Delta^{++}\pi^-\pi^0$ final states. The number removed in either case amounted to less than 15% of the original sample of events. Figure 2(a) shows the $\pi^+\pi^-$ mass spectra for all events for which the angle ($\theta_{\pi p}$) between the incident π^+ and outgoing proton in the π^+n center of mass satisfies the condition $\cos\theta_{\pi p} \geq 0.7$ and $\cos\theta_{\pi p} \geq 0.9$. Figure 2(b) shows the angular distribution for $\theta_{\pi p}$. There is evidently a sharp forward peaking of the proton that is approximately independent of the $\pi^+\pi^-$ mass. The shape of the Cherenkov counter C_2 used in the trigger requirement introduces geometrical restrictions on the angular acceptance for the forward protons. The corrected angular distribution for Reaction (1) is shown in Fig. 2(a) and is denoted by dashed lines. For $\cos\theta_{\pi p} > 0.95$ the corrections are seen to be negligible. Figure 2(c) shows the $\pi^+\pi^-\pi^0$ mass distribution for Reaction (2) for the cuts $\cos\theta_{\pi p} \geq 0.7$ and $\cos\theta_{\pi p} \geq 0.9$. The corresponding angular distribution for $\theta_{\pi p}$ is shown in Fig. 2(d). Again a relatively sharp forward peaking of the proton is observed.

The di-pion and tri-pion mass distributions shown in Figs. 2(a) and 2(c) are from the same sample of film. The most striking features of the $\pi^+\pi^-\pi^0$ mass spectrum are the strong ω signal (centered at ~ 780 MeV), the negligible η signal (~ 4 events near 550 MeV), and the possible further structure in the mass plot in the mass range 975-1100 MeV.^{4,5} The striking ω peak in Fig. 2(c) especially for the $\cos\theta_{\pi p} \geq 0.9$ cut as mentioned previously provides evidence for the clean separation of Reaction (2) from the background. The mass resolution for the $\pi^+\pi^-\pi^0$ final state at the ω mass appears to be approximately 75-100 MeV, which is reasonable considering the size of the bubble chamber and the low constraint class for Reaction (2). The insert in Fig. 2(d) shows the $\theta_{\pi p}$ angular distribution for events pro-

duced in the ω peak (675-825 MeV). The production cross section for the $\cos\theta_{\pi p} \geq 0.98$ is $\sim 150 \mu\text{b/sr}$.

The structure near 1 BeV in the 3π mass spectrum is suggestive of similar structure in $\pi^+\pi^-\pi^0$

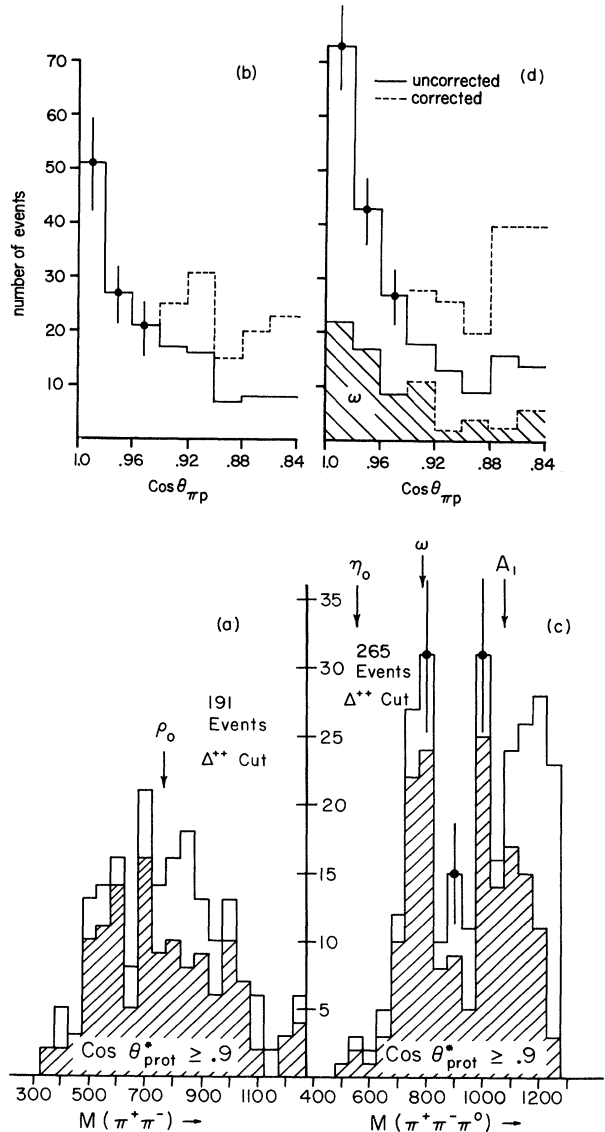


FIG. 2. (a) The $\pi^+\pi^-$ mass distribution for events of Reaction (1) with $\cos\theta_{\pi p} \geq 0.7$. The cross hatched events have $\cos\theta_{\pi p} \geq 0.9$. (b) The angular distribution of the proton relative to the incident π^+ in the π^+n center of mass for Reaction (1). The dashed lines represent the corrected data. (c) The $\pi^+\pi^-\pi^0$ mass distribution for events of Reaction (2) with $\cos\theta_{\pi p} \geq 0.7$. The cross hatched events have $\cos\theta_{\pi p} \geq 0.9$. (d) The angular distribution of the proton relative to π^+ in the π^+n center of mass for events of Reaction (2). The cross-hatched events represent the angular distribution for ω production. The dashed lines represent the data with geometrical corrections included.

observed recently.⁶ However, in our experiment this structure, while intriguing, is not yet statistically compelling. We have also searched for the reaction

$$\pi^+n \rightarrow K^+K^-p(\pi^+d \rightarrow K^+K^-pp) \quad (3)$$

for $\cos\theta_{\pi p} \geq 0.7$. No events were observed in the same sample of film represented by the number of events shown in Figs. 2(a) and 2(c). Backward φ production would be observed through Reaction (3) and, therefore, the φ production is strongly suppressed relative to backward ω production.⁷ The φ decay into three pions contributes less than one event to the 1-BeV enhancement in Fig. 2(c). A similar conclusion holds for η' production and decay into $\pi^+\pi^-\gamma$.

The $\pi^+\pi^-$ mass spectrum appears more anomalous. In particular, there is no direct evidence for the production of the ρ^0 from the mass plot in contrast to the strong production of the ω mentioned above.⁸ It should be recalled that in π -meson exchange reactions with the $\pi^+\pi^-$ final state being produced, a dominant ρ signal is observed centered at a mass of 765 MeV and falling by at least a factor of 5 at the mass value of 600 MeV.⁹ In contrast the $\pi^+\pi^-$ mass spectrum shown in Fig. 2(a) appears to rise (for $\cos\theta_{\pi p} \geq 0.9$) in going from 765- to 600-MeV di-pion mass. The effect is suggestive of a vastly different production mechanism for $\pi^+\pi^-$ events produced near 180° from those produced near 0° relative to the direction of the incident π meson. This is not to say that the ρ^0 is not produced in the former processes, but only that the background under the ρ may be greatly different in the two cases. The possibility of interference between ρ and the background resulting in a distorted mass spectrum cannot be ruled out.

In order to investigate the di-pion final state further the $\pi\pi$ angular correlations have been recorded. Figure 3(a) shows the coordinate system used (u -channel coordinate system). The di-pion production is presumed to proceed through baryon exchange so that at the $\pi\pi$ vertex the $\bar{N}N$ annihilation process $\bar{N}N \rightarrow \pi\pi$ occurs. The definitions of $\theta_{\pi\pi}$, the scattering angle between the incident nucleon and the outgoing π^+ in the di-pion rest frame, and φ , the Treiman-Yang angle, are completely analogous to those used in meson-exchange reactions. In order to enhance the probability for baryon-exchange dominance of Reaction (1) the $\pi\pi$ angular correlations studies are restricted to $\cos\theta_{\pi p} \geq 0.9$. Figure 3(b) shows the angular distribution of $\theta_{\pi\pi}$ for all di-pion

masses. The distribution is consistent with isotropy. Figure 3(c) shows the Treiman-Yang angle distribution. This distribution is not consistent with isotropy. Finally, the forward-backward and polar-equatorial ratios for the $\theta_{\pi\pi}$ distribution as a function of di-pion mass are recorded in Figs. 3(d) and 3(e). The $(P-E)/(P+E)$ ratios are consistent with zero below 1-BeV di-pion mass but appear to deviate becoming positive in the mass range 1100-1300 MeV. The $(F-B)/F+B$ ratio is definitely nonzero below 1 BeV, first being negative at low $\pi\pi$ mass, and passing through zero in the mass range of 650-750 MeV. This behavior is suggestive of an interference between the $\pi\pi$ background and the ρ ,

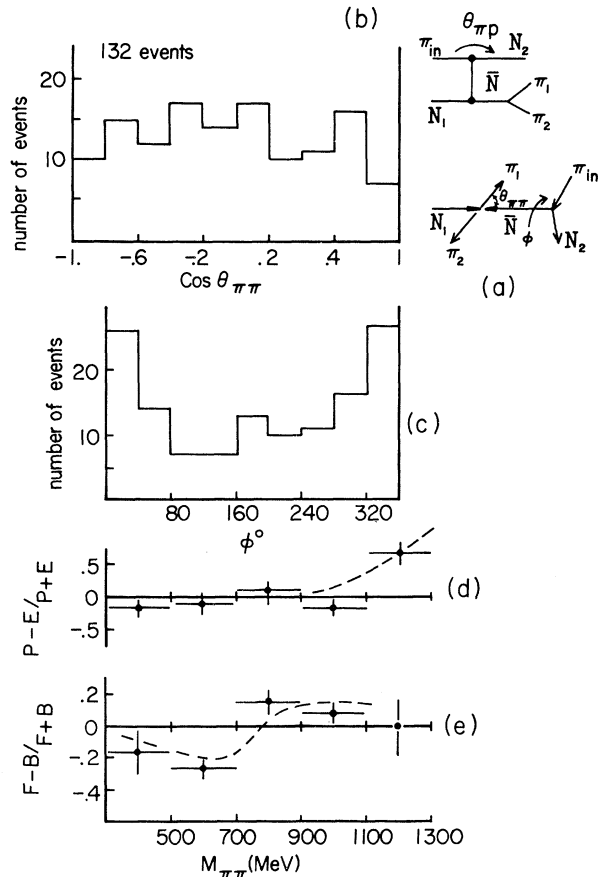


FIG. 3. $\pi\pi$ decay correlations. (a) The production process assumed to dominate Reaction (1) for $\cos\theta_{\pi p} \geq 0.9$ and the u -channel coordinate system. φ is the Treiman-Yang angle and $\theta_{\pi\pi}$ is the scattering angle between the outgoing π^+ and incident nucleon (N_1) in the $\pi\pi$ center of mass. N_2 is the final-state proton. (b) The angular distribution of $\theta_{\pi\pi}$. (c) Treiman-Yang angular distribution. (d) The polar-equatorial ratio of the $\theta_{\pi\pi}$ distribution. (e) The forward-backward ratio of the $\theta_{\pi\pi}$ distribution.

the interference changing sign approximately in the mass range of the ρ .

A preliminary interpretation of the $\pi\pi$ angular distributions can be given on the basis of a baryon-exchange model for Reaction (1). The production of di-pions in Reaction (1) is assumed to proceed via the process

$$\bar{N}N \rightarrow \pi^+\pi^- \quad (4)$$

at the di-pion vertex. Assuming spin- $\frac{1}{2}$ unpolarized baryon exchange the $\theta_{\pi\pi}$ angular distribution is given by¹⁰

$$N(\theta_{\pi\pi}) = 3|S_1'|^2 + \frac{2}{3}|P_1^0|^2 + 2\sqrt{2}\cos\theta_{\pi\pi}\text{Re}S_1'P_1^0, \quad (5)$$

where A_K^J refers to the S-matrix element for process (4), corresponding to the A orbital-momentum state of the $\bar{N}N$ system with K as the spin of the $\bar{N}N$ system and l the orbital angular momentum of the di-pion system. In expression (5) only the 3S_1 and 3P_0 $\bar{N}N$ states have been included with the assumption being made that higher angular-momentum states are suppressed by the centrifugal barrier.

On the basis of this model the small $(P-E)/(P+E)$ ratios shown in Fig. 3(d) suggest the dominance of first term in Eq. (5), i.e., the dominance of either the $l=1$ or $l=0$ final state or both. Furthermore, the behavior of the $(F-B)/(F+B)$ ratio suggests that the second term in Eq. (5) changes sign at the ρ mass. Finally, the increase of the $(P-E)/(P+E)$ ratio above 1100 MeV suggests that higher angular-momentum states become important above 1100 MeV. These speculations suggest a simple but possibly nonunique physical picture of the process (4) where the low-mass region is dominated by the production of a broad $l=0$, $T=0$ $\pi\pi$ state, the ϵ , with ρ production being considerably weaker, and with the production of the f^0 becoming important above 1100 MeV. The nonisotropy of the φ distribution in Fig. 3(c) is not inconsistent with this picture. The absence of any strong ρ signal in the mass plot [Fig. 2(a)] is also consistent with such a model. This model would require that the ϵ be considerably wider than the ρ , which is in agreement with recent studies of the reaction $\pi^+n \rightarrow \pi^0\pi^0p$ at 2.15 BeV/c.^{10,11} The dominance of the ϵ over the ρ in Reaction (4) does not disagree with any theory or experiment known to us. Furthermore, backward dispersion analyses require a sizeable coupling of the ϵ in Reaction (4).¹²

We wish to thank Professor V. Hagopian and Dr. H. Kautzky for help with the setting up of this experiment and the excellent running of the Princeton-Pennsylvania Accelerator bubble chamber. The help of Professor U. Camerini, D. Clarke, R. Rutz, T. Ling, and J. Mapp is also acknowledged. We also thank Dr. B. Cork, Dr. W. Wenzel, and Dr. W. Chen for the loan of some Cherenkov counters and Professor L. Pondrom for the loan of equipment. Finally we thank the Wisconsin scanning and measuring staff for their help.

*Work supported in part by the U. S. Atomic Energy Commission under Contracts No. AT(11-1)-881, COO-881-253.

†Accepted without review under policy announced in Editorial of 20 July 1964 [Phys. Rev. Letters **13**, 79 (1964)].

‡Alfred P. Sloan Fellow (1968-1970).

§On leave from Tata Institute of Fundamental Research, Bombay 5, India.

¹M. Bazin *et al.*, Princeton-Pennsylvania Accelerator Report No. PPAD 2137-561 (unpublished).

²T. B. Day, University of Maryland Report No. 649 (unpublished).

³The production of the $\Delta^{++}\pi^-$ (or $\Delta^-\pi^+$) final state at this beam energy with low momentum transfer between the beam pion and the Δ^{++} (or Δ^-) has been previously observed by R. Anthony, C. Coffin, E. Marley, J. Rice, N. Stanton, and K. Terwilliger, Phys. Rev. Letters **21**, 1605 (1968).

⁴The upper limit on the ratio backward $\pi^+n \rightarrow p\eta$ to backward $\pi^+p \rightarrow p\pi^+$ for $\cos\theta > 0.9$ is found to be 0.4 ± 0.3 . This ratio is consistent with N_α exchange dominance for these two reactions assuming an $F/(F+D)$ ratio of $\sim \frac{2}{3}$ as predicted by SU(6).

⁵See also E. W. Anderson *et al.*, Phys. Rev. Letters **22**, 1390 (1969).

⁶D. J. Crennell *et al.*, Phys. Rev. Letters **22**, 1398 (1969), and also an unpublished Wisconsin experiment (D. D. Reeder, private communication).

⁷Such a suppression has been previously observed in K^+p reactions and is consistent with the expectations of SU(6) and the quark model. See, for example, J. Mott *et al.*, Phys. Rev. Letters **18**, 355 (1967).

⁸Evidence for backward-hemisphere ρ^0 production in the reaction $\pi^-p \rightarrow \pi^+\pi^-n$ at 4 BeV/c has been obtained in a Notre Dame-Purdue-Stanford Linear Accelerator Center collaboration. However, their angular bins were much less restrictive than the ones used here (Z. G. T. Guiragossian, private communication).

⁹See, for example, E. West, J. Boyd, A. Erwin, and W. D. Walker, Phys. Rev. **149**, 1089 (1966).

¹⁰R. J. N. Phillips, Nucl. Phys. **25**, 348 (1961).

¹¹J. Braun, D. Cline, and V. Scherer, Phys. Rev. Letters **21**, 1275 (1968); J. Smith and G. Manning, Phys. Rev. **171**, 1399 (1968).

¹²W. D. Walker, in Proceedings of a Conference on the

$\pi\pi$ and $K\pi$ Interactions, Argonne National Laboratory,
14-16 May 1969 (unpublished).

¹³C. Lovelace, CERN Report No. TH 839, and private
communication.

X-RAY TRANSITION RADIATION APPLIED TO THE DETECTION OF SUPERHIGH-ENERGY PARTICLES*

Luke C. L. Yuan and C. L. Wang
Brookhaven National Laboratory, Upton, New York 11973

and

S. Prunster
Argonne National Laboratory Argonne, Illinois 60439
(Received 10 July 1969)

Preliminary measurements of the transition radiation in the x-ray region indicate that an average of 12 x-ray photons are produced by a single positron of 2-BeV energy traversing a stack of 231 thin aluminum foils. This number is large enough to indicate that it is feasible to use the x-ray transition radiation for the determination of the relativistic factor γ rather than β of superhigh-energy particles. Such an application may well provide a unique method for distinguishing monoenergetic particles in the superhigh-energy region.

In our earlier work^{1,2} we have measured the transition radiation emitted in the optical region by individual charged protons, pions, and electrons in the momentum region 0.8-3.5 BeV/c with the value of γ ranging from 1 up to 2000, where $\gamma = (1 - \beta^2)^{-1/2}$. We have also established the log γ dependence of the intensity of the transition radiation in the optical region as predicted by theory.³ By limiting the detection of the optical transition radiation emitted within a small angular region around the direction of the incident particle a much stronger γ dependence has been observed.⁴⁻⁶

Theory³ also predicted that the intensity of the transition radiation in the x-ray region is linearly proportional to γ . This linear dependence arises from the combined effect of two separate factors, namely, (i) the increase with γ in the magnitude of the energy distribution of the transition radiation as a function of frequency and (ii) the increase with γ in the frequency range of the transition radiation. This would provide an adequately sensitive γ dependence for its application to the detection and identification of individual, charged particles in the superhigh-energy region.

Recently we have carried out an experiment to measure the transition radiation emitted in the x-ray region by individual positrons at the 6-BeV Cambridge Electron Accelerator. This paper describes some of the preliminary results obtained in this experiment.

The experimental arrangement is comprised of a beam-defining scintillation-counter telescope

in front of a transition radiator (a stack of thin foils closely spaced). Immediately following the transition radiator is a bending magnet which deflects the positrons into a scintillation counter placed downstream of the magnet on one side. The x-ray transition radiation is measured by a lithium-drifted germanium detector placed also downstream of the deflection magnet.

The coincidence signal from each positron passing through the beam-defining telescope and the scintillation counter downstream of the magnet opens the gate in a linear gate circuit which allows the registration of the x-ray pulses from the germanium detector. Figure 1 shows the intensity of the radiation detected versus its energy. The peak at the left is due to the "pedestal" pulses from the incident-positron signals which serve to define the zero signal level as well as for normalization purposes. The range of the radiation energy detected in the preliminary measurements extends from 6 to 200 keV as calibrated with a known source. The vertical scale gives the relative intensity in a logarithmic scale. The lower curve shows the background radiation obtained by replacing the transition radiator by a solid block of the same mass and material as the whole stack of foils but without the multitude of interfaces. The background radiation is mainly comprised of bremsstrahlung from the incident high-energy positrons, which would be very small for protons and other heavier particles. Other possible effects caused by the bending of the positron in traversing a magnetic field which might contri-